AN IMPROVEMENT OF THE TIME DELAYED QUASI-STEADY MODEL FOR THE OSCILLATIONS OF CIRCULAR CYLINDERS IN CROSS-FLOW

P. Hémon

Institut Aérotechnique/CNAM, 15, rue Marat, F-78210 Saint-Cyr-l'Ecole, France

This paper is devoted to an improvement of the time-delayed quasi-steady model for the prediction of the movement-induced vibrations of tubes mounted in tandem or in an in-line bundle. The improvement lies in the physical interpretation and calculation of the time lag which is based on measured steady force coefficients. In order to calculate the time lag, a mean convection velocity between cylinders is estimated at each time step. A linear analysis of the present model gives a critical velocity which is in good agreement with an unsteady experiment found in the literature. Moreover, limit-cycle amplitudes are relatively well predicted and show that instability is triggered by the time lag, whereas amplitude is governed by nonlinear aerodynamic damping as for a Van der Pol oscillator. © 1999 Academic Press

1. INTRODUCTION

FLOW-INDUCED VIBRATIONS of cylinders mounted in bundles is an important engineering problem in many industrial fields. Actually, one can find many different situations where such vibrations may occur when the cylinders are subjected to cross-flow. Examples are the effect of wind on in-line chimney stacks, on electric power-line bundles and on the cables of suspended bridges, or the effect of sea currents on offshore structures and on risers, and also the effect of confined and complex flows in reactors of nuclear power plants and in conventional heat exchangers.

Two kinds of physical phenomena are classically found: the vortex-shedding excitation due to the so-called Bénard–Karman street, and the motion-induced vibrations often denoted as galloping, wake galloping or interference galloping, according to the aero-hydrodynamic configuration of the problem. This paper is concerned with the second kind of instability, without any interaction with the first.

Bokaian & Geoola (1984) carried out many experiments with simplified configurations of two cylinders subjected to cross-flow: some typical amplitudes of oscillation of the leeward cylinder are given in Figure 1 for the case of a tandem arrangement and with the windward cylinder fixed. The set-up did not allow oscillations in the longitudinal direction. Both types of instability are present. Though for large spacing ratios (L/D) one can see that the two phenomena are not coupled, this is not true for cylinders that are close. When the cylinders are closer than the case shown in figure, the phenomena are completely merged.

From an engineering point of view, it is easy to identify the risk of vortex-induced instability because it is mainly governed by a resonance effect between the bending frequency of the cylinder and the frequency of vortex shedding. The quantitative prediction of the oscillations are nevertheless more complex because of the lock-in problem.
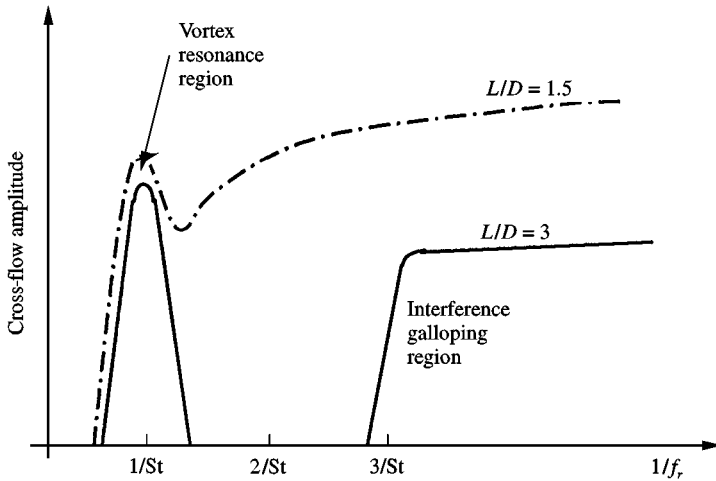
Figure 1. Typical cross-flow response of the leeward cylinder of two tubes in a tandem arrangement.

Concering motion-induced oscillations, however, the identification of the risk of instability remains unresolved with simplified methods. However, many models have been developed over the years and some of them have now became classical.

1.1. Short Review of Classical Models

In most cases, cylinders are free to vibrate transversely in their two coordinate directions, in flow (x) and cross-flow (y), representing two degrees of freedom (DOF). The pioneering work of Theodorsen (Fung 1955) and Küssner was the study of the problem of the sinusoidal torsion and bending oscillations of a wing profile. A similar model adapted to the wake galloping problem of electric power lines was suggested by Simpson and is reported in Simiu & Scanlan (1986). This model can be written as

$$m\ddot{x} + c_x\dot{x} + k_x x + k_{xy}y = \tfrac{1}{2}\rho V^2 D(A_1 x + A_2 y + A_3\dot{x} + A_4\dot{y}),$$
$$m\ddot{y} + c_y\dot{y} + k_y y + k_{yx}x = \tfrac{1}{2}\rho V^2 D(B_1 x + B_2 y + B_3\dot{x} + B_4\dot{y}), \tag{1}$$

where the structural stiffness and damping are k and c, respectively, for each degree of freedom and their coupling. Simpson's model calculates the coefficients A_i and B_i ($i = 1$–4) by using the static aerodynamic coefficients of the leeward cylinder and the mean velocity in the wake of the windward cylinder. It is a pure quasi-steady theory, and comparison with experiments is satisfactory for a staggered configuration and a spacing ratio (L/D) greater than 5.

The model is linear and can only detect the boundaries of the stability region. It has common points with Theodorsen's model, even if the problems and the degrees of freedom are different. Indeed, Theodorsen used an unsteady potential flow theory for the calculation of the coefficients in the aeroelastic force model. In the 1970s, Scanlan (Simiu & Scanlan 1986) introduced the flutter derivatives model for studying bridge deck sections. These derivatives are similar to the previous coefficients and are estimated through unsteady tests in wind tunnel.

A number of other authors have developed different methods for predicting galloping in arrays of cylinders. Many of them have based their models on the use of unsteady

coefficients obtained through unsteady wind tunnel experiments. Recently, Chabart & Lilien (1997) carried out a large number of tests for electric power lines with a view to numerical code validation and also more practical applications such as the design of control system.

Numerical modelling represents an alternative to unsteady wind tunnel testing. The work of Blazik-Borowa & Flaga (1997) is an interesting example of this, because the authors studied the effects of turbulence intensity and Scruton number with a nonlinear quasi-steady model of their own. Also, Kern & Maitz (1997) derived a nonlinear analysis of a conventional quasi-steady model with the help of the normal form theory.

1.2. INTRODUCTION TO TIME DELAYED QUASI-STEADY MODEL

The above-mentioned researchers made the assumption that the time lag, i.e. the delay between aeroelastic force and body displacement, is negligible. However, it has been reported by many other authors that, for certain configurations, the time lag cannot be neglected because this delay is the trigger of the transfer of energy from the flow to the structure (Dielen & Ruscheweyh 1995; Granger & De Langre 1995; Granger & Païdoussis 1996; Knisely & Kawagoe 1988). This problem mainly concerns the vibration of tube arrays, where the spacing ratio is often smaller than the one encountered in electric power lines or cables.

The reduced frequency is assumed to be small and the oscillation amplitudes are assumed to be within the linear elastic range of the structures. Moreover, such oscillations are mainly in the cross-flow direction so that some models neglect the longitudinal movement.

A quasi-steady method is based on steady tests in which the aerodynamic coefficients of the tubes are measured in different positions and are used in a model which is solved numerically. These experiments are easy to perform by comparison with unsteady tests. However, the great disadvantage is that the dynamic effect on the coefficients is missing because they are measured on motionless tubes, whereas in reality they move. The computational model must compensate for this, which means that unsteady effects need to be introduced.

Granger & Païdoussis (1996) have suggested such an improvement of the quasi-steady model: they used an impulsive function of the cylinder motion to develop what they called a quasi-unsteady model where very few empirical parameters have to be determined through dynamic tests. Their model is considered as a generalization of the Price & Païdoussis (1984) model which introduces the time lag in an intuitive manner.

Indeed, the so-called Price & Païdoussis model is an interesting way to obtain good qualitative results by comparison with experiments. This model assumes that the behaviour of a tube can be described by the dynamics equations

$$m\ddot{x}(t) + 2\eta\omega m\dot{x}(t) + m\omega^2 x(t) = F_x(x(t-\tau), y(t-\tau), \dot{x}(t), \dot{y}(t)),$$

$$m\ddot{y}(t) + 2\eta\omega m\dot{y}(t) + m\omega^2 y(t) = F_y(x(t-\tau), y(t-\tau), \dot{x}(t), \dot{y}(t)),$$

(2)

where x and y denote the along-wind and cross-wind displacements of the tube and F_x and F_y are the corresponding components of the aeroelastic force which is a function of the displacement and of the velocity of the cylinder. When the tube moves, the aeroelastic force changes with a little time lag τ, because the viscous flow is not restored instantaneously. In fact, this time lag is a key element of the model because it is impossible to simulate an instability without it, even when oscillations are observed experimentally. The Price

& Païdoussis model assumes that the time lag is a characteristic time scale of the flow and is given by

$$\tau = \mu \frac{D}{V}, \tag{3}$$

where μ is a dimensionless parameter close to 1. However, this expression is rather simple and difficult to link with a time response of the flow. Moreover, it was experimentally shown (Dielen & Ruscheweyh 1995) that τ depends on the tube position during its oscillations, which is not reproduced in expression (3).

The main purpose of the present paper is to suggest an improvement to the formulation of the time lag by avoiding empirical parameters such as μ. The object of this study was initially aimed at heat exchangers. The external fluid is assumed to be air so that added mass effects are neglected. The tubes must be able to withstand thermal expansion effects and are therefore mounted very flexibly which makes them very sensitive to vibrations.

First, a presentation of a quasi-steady model is given. This model is then applied to the cases of two cylinders in tandem and an in-line tube bundle (see Figure 2). The description of a new expression for the time lag follows. Some results of the experimental study performed on fixed rigid tubes are then given and used as input to the present model for numerical predictions. Comparisons are made with available unsteady experimental results and the quasi-steady assumption is replaced in the context of the present model.
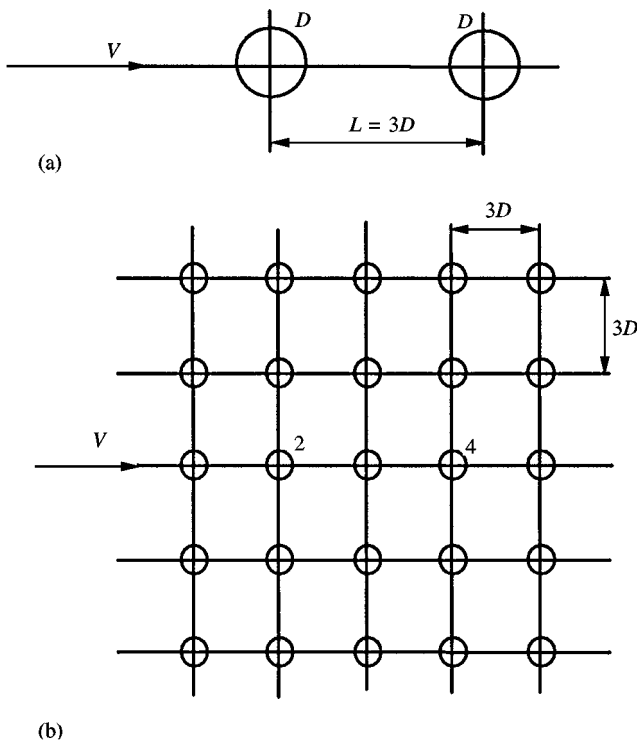
Figure 2. Sketch of the two cases studied: (a) two cylinders in tandem; (b) in-line tube bundle.

2. THE QUASI-STEADY MODEL

2.1. PRESENTATION OF THE MODEL

The model presented, initially shown in Hémon (1997), is based on the assumption that the steady aerodynamic force coefficients are known for different positions of the tubes through experiments or numerical predictions. In the present case, the distance L between the tubes is equal to 3 times their diameter D. Zdravkovich (1987) made a extensive review of the different possibilities of oscillations in many configurations and presents a possible proximity and wake galloping instability for the present case ($L/D = 3$).

An important point in a pure quasi-steady theory is the fact that the dynamics of the flow due to the cylinder movement are neglected. Though experimental studies (Chen 1987) show that the oscillating leeward cylinder drags the wake of the windward cylinder (Figure 3), the assumption is obviously valid when the displacement of the tube remains small and it is used for the present model.

The main purpose of the modelling is to reproduce the movement dependence of the aeroelastic force, i.e. the force must depend on the displacement (x, y) and on the velocity $(\dot{x}, \dot{y})$. A very convenient simplification, especially for experiments, is to consider once again limited amplitudes of oscillation so as to reduce the displacement (x, y) to the angle β_p, as defined in Figure 4. This angle is given by

$$\tan \beta_p = \frac{y}{L + x},\tag{4}$$

and is denoted as the yaw angle of the axis joining the two tubes. Though the sketch of Figure 4 neglects the along-wind displacement for the sake of clarity, expressions (4)–(6) are for the two-degree-of-freedom case. We now have the aerodynamic force coefficients as a function of the angle β_p instead of position (x, y). The aeroelastic force can then be
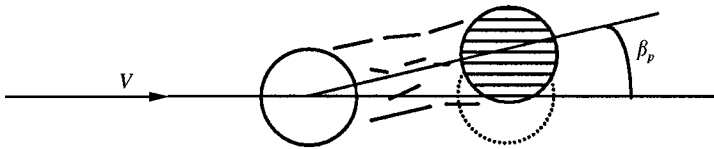
Figure 3. Wake dragged by the movement of the downstream cylinder.
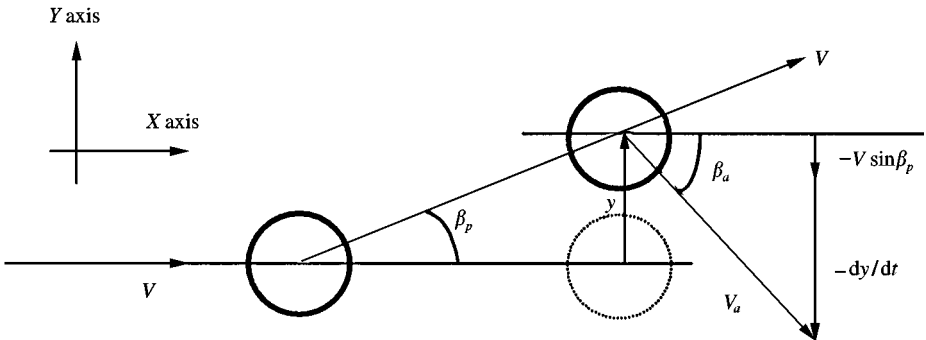
Figure 4. Definition of angles and velocities.

expressed in a general form by

$$F_x(x(t-\tau), y(t-\tau), \dot{x}(t), \dot{y}(t)) = \tfrac{1}{2}\rho D V_a^2 C_x(\beta_a),$$

$$F_y(x(t-\tau), y(t-\tau), \dot{x}(t), \dot{y}(t)) = \tfrac{1}{2}\rho D V_a^2 C_y(\beta_a),$$

(5)

since the viscous stress component is neglected for such bluff bodies. The drag and lift force coefficients depend on the relative yaw angle β_a (see Figure 4) which is defined with the relative velocity V_a due to the oscillation velocity of the tube. In order to complete the model,

$$V_a^2 = (V\cos\beta_p - \dot{x})^2 + (V\sin\beta_p + \dot{y})^2,$$

$$\tan\beta_a = -\frac{V\sin\beta_p + \dot{y}}{V\cos\beta_p - \dot{x}}.$$

(6)

This model is quite complex because it takes into account (i) the tube displacement referred to the upstream cylinder, which effectively creates large force variations, and (ii) the relative wind velocity which introduces a coupling with the velocity of the structure.

For the remainder of this paper, the along-wind displacement will be neglected. The unsteady experiments that are used for the validation of the model considered only a single degree of freedom. In that particular case, the along-wind degree of freedom was not found to be of great importance, but the extension to other applications, especially with larger cylinder spacing ratios, should not be restricted to the cross-flow movement.

The geometrical approximation made by equation (4) introduces an error, Δy, on the displacement y: this increases when the angle β increases and when L decreases. For an angle of $18.4°$, corresponding to a cross-flow displacement of one diameter, the error in the displacement reaches 5.1% of the diameter. For the linearized model of the aeroelastic force, the corresponding error is doubled.

Furthermore, it is possible to add the effect of the displacement of the upstream tube by modifying expression (4). If we assume that the movements of the tubes occur out of phase, then one can write

$$\tan\beta_p = \frac{y + y_u}{L + x + x_u},$$

(7)

where (x_u, y_u) denotes the displacement of the upstream tube. However, this relationship will not be used in the present paper since it depends strongly on tube spacing and on the assumption of an out-of-phase movement.

2.2. LINEAR ANALYSIS OF THE DYNAMICAL SYSTEM

For cross-flow vibrations, the critical velocity can be estimated by linearizing the model and by making an energy balance over a period T of the movement, assuming that it is periodic, with an angular velocity ω. We use the expansion of the force to the first order,

$$F_y(y(t-\tau), \dot{y}(t)) = F_{y_0} + \frac{\partial F_{y_0}}{\partial y}(y(t-\tau) - y_0) + \frac{\partial F_{y_0}}{\partial \dot{y}}(\dot{y}(t) - \dot{y}_0),$$

(8)

where subscript 0 refers to functions evaluated for the equilibrium position $(y_0, \dot{y}_0)$. It is convenient to use a steady equilibrium position such that $\dot{y}_0 = 0$, which is compatible with the quasi-steady assumption. This expansion is introduced into the dynamics equation (2)

to make the energy balance over a period, such that

$$m[E_C + E_p]_0^T = \Delta E_S + \Delta E_d,$$

with

$$\Delta E_S = \int_0^T \frac{\partial F_{y_0}}{\partial y} \left(y(t - \tau) - y_0 \right) \dot{y}(t) \, dt,$$

$$\Delta E_d = \int_0^T \left(\frac{\partial F_{y_0}}{\partial \dot{y}} - 2\eta \omega m \right) \dot{y}^2(t) \, dt,$$

(9)

where E_C and E_p are the kinetic and potential energies, respectively. The balance introduces two nonconservative components ΔE_S and ΔE_d related to aerodynamic stiffness and damping, respectively. When the energy balance is positive, an instability can occur. If it is negative, the dynamical system is stable. It is important to note here that if the time lag is neglected, the stiffness term becomes nil and an instability can appear only through aerodynamic damping.

We then assume that the movement is sinusoidal,

$$y(t) = y_M \sin(\omega t),$$

(10)

and we can integrate the nonconservative terms. After calculations and the introduction of the force derivatives, the equilibrium position being the perfectly aligned tube ($y_0 = 0$), one obtains

$$\Delta E_S = \tfrac{1}{2} \rho D V^2 \frac{1}{L} \frac{\partial C_{y_0}}{\partial \beta} y_M^2 \sin\left(2\pi \frac{f_r}{\tau_r} \right),$$

$$\Delta E_d = -\left(\frac{1}{2} \rho D V \frac{\partial C_{y_0}}{\partial \beta} + 2\eta \omega m \right) y_M^2 \pi \omega,$$

(11)

where f_r is the reduced frequency and τ_r the reduced time lag (see Appendix 2). The critical velocity is defined as the velocity which makes the system unstable, i.e. when the energy balance becomes positive.

These expressions show qualitatively that, knowing that the lift gradient in a tandem arrangement is positive, the damping part of the energy balance cannot lead to instability. This can only happen when the term $\sin(2\pi f_r / \tau_r)$ becomes positive. Blevins (1990) reported that the time lag is of the order of the Strouhal number, and we temporarily take this value. Also see Figure 1 for clarifying references to the reduced frequency. One concludes that

(i) when f_r is close to St (also to τ_r), the sinus term is close to zero and no instability can occur;

(ii) when f_r decreases (the velocity increases) down to $\tfrac{1}{2}\tau_r$, the sinus term is negative again and the system remains stable;

(iii) if the velocity further increases, one reaches the region where $f_r < \tfrac{1}{2}\tau_r$, the sinus term becomes positive and an instability can develop as observed in experiments.

These conclusions were drawn on the basis that the time lag was taken to be constant, which in reality is not the case. An expression of the time lag introducing a dependence on the velocity of the flow will be given in the third part of this paper. However, the above linear analysis leads to a useful estimation of the critical velocity.

2.3. Critical Velocity Estimation

Starting from expressions (11), we obtain an implicit solution of the critical velocity, which is easily solved by any numerical procedure:

$$V_{r_{cr}} = \frac{1}{f_{r_{cr}}} = \frac{L}{D} \frac{\pi}{\sin(2\pi f_r/\tau_r)} \left(1 + \sqrt{1 + 8Sc \frac{D}{L} \frac{\sin(2\pi f_r/\tau_r)}{\partial C_{y_0}/\partial \beta}} \right), \tag{12}$$

where subscript cr refers to critical values and Sc is the Scruton number. The critical velocity appears to be a function of the square root of the Scruton number, which is a well-known result. We do not make any assumption concerning the sign of the gradient of the lift force, but the solution is supposed to exist and the component under the square-root is assumed positive.

It is therefore quite difficult to compare this expression with the one given by Dielen & Ruscheweyh (1995), because they assumed a negative gradient of the lift force. In fact, as shown in Figure 5, the lift force has a positive slope when the cylinders are in alignment (except for tube 4 of the bundle studied), and a negative slope when they are staggered. In the latter case, if we consider an equilibrium position different from the alignment, i.e. y_0 is not zero, the expression obtained is much more complex:

$$V_{r_{cr}} = \frac{L^2 + y_0^2}{LD} \frac{\pi(2C_{y_0}(y_0/L) + \partial C_{y_0}/\partial \beta)}{(\partial C_{y_0}/\partial \beta)\sin(2\pi f_r/\tau_r)} \left(1 + \sqrt{1 + 8Sc \frac{LD}{L^2 + y_0^2} \frac{(\partial C_{y_0}/\partial \beta)\sin(2\pi f_r/\tau_r)}{(2C_{y_0}(y_0/L) + \partial C_{y_0}/\partial \beta)}} \right). \tag{13}$$

Henceforth in this paper we shall consider only in-line tubes.

From expression (11) we have seen that the existence of an instability is also a function of the value of the time lag which has not been detailed yet. The single criterion of instability based on the gradient of the lift force is shown to be insufficient. The classical definition initially derived by Den Hartog (1934), of a stable system given by a positive slope, and an unstable one by negative gradient, is clearly wrong in the case of aligned tubes, because the time lag effects calls into question the quasi-steady assumption.

3. THE IMPROVED TIME LAG CALCULATION

The time lag is the delay between the aeroelastic force and the displacement of the tube generating it. This is the time taken by the flow to adapt itself to the new configuration induced by the movement of the tube.

In this model, the displacement of the tube is obtained with reference to the upstream tube, using the angle β_p. This upstream tube creates the interference which induces the lift force variations on the downstream cylinder. However, as interference is not transmitted instantaneously, there is an implicit time lag. Therefore, this delay should be understood as a convection time of the mean flow between tubes, i.e.

$$\tau = \frac{L}{U_C}, \tag{14}$$

where U_C is a convection velocity between the two tubes inside the wake of the upstream tube. It is obvious that this velocity is not a constant if the downstream tube moves, because it periodically goes in and out of the wake of the upstream cylinder. The region where this movement occurs is characterised by a very high gradient of the mean velocity; in particular, the moving tube regularly crosses the shear layer which is reinforced in the case of bundles.

The flow in such cases is so complex that it cannot be solved numerically, and an experimental measurement of this velocity is not easy to perform because of the intrusion of a velocity sensor. However, we have assumed that the force coefficients of the tubes are known as a function of the yaw angle and we can also assume that the force coefficient C_{x_M} of an isolated tube is known as a reference value.

An estimation of the mean velocity U_C can then be given with reference to the case of an isolated cylinder, so that one has

$$\frac{U_C^2(\beta_p)}{\sqrt{C_x^2(\beta_p) + C_y^2(\beta_p)}} = \frac{V^2}{C_{x_M}}, \tag{15}$$

where the coefficients C_x and C_y are the drag and lift coefficients, respectively, of the downstream tube. The great advantage of the calculation suggested here is that there is no empirical coefficient to adjust and there is not need for other data than those already known.

4. EXPERIMENTAL STUDY

In order to validate the model, the two cases presented in Figure 2 were studied and especially the case of two cylinders placed in tandem for which the results of unsteady experiments are available (Bokaian & Geoola 1984).

The data which are necessary as input for the aeroelastic force model are the force coefficients versus the yaw angle. These data were obtained in a facility at the Institut Aéro Technique (IAT) adapted to high turbulence flows such as those found in heat exchangers. The square test-section has 0·6 m sides and the velocity can be varied from 5 to 40 m/s. The turbulence intensity measured at the entrance to the test-section is 5%. The diameter of the tubes was 40 mm and the Reynolds number of tests was 51 000, based on the upstream velocity. For the bundle, the Reynolds number based on the velocity between two rows reached 71 000.

Two high-frequency response pressure transducers (ENDEVCO) were flush mounted at the surface of two cylinder elements. Each of these could be moved to different spanwise positions of the two cylinders, thus allowing certain correlation measurements. The transducers were connected to appropriate electronic devices and to a high speed analog/digital converter in a computer (PC). The data transferred to a Unix workstation for signal processing and pressure integration. The experimental procedure was checked on an isolated cylinder by comparison with well known results from the literature (pressure distribution/C_{x_M} = 1·271/St = 0·190/span-wise correlation length of vortex shedding equal to 3D).

Figure 5 presents the steady lift coefficients of the three tubes studied, obtained through integration of the pressure measurements. The curves have been smoothed using a least-squares method. Figures 6–8 give some typical pressure profiles obtained, in terms of the mean pressure coefficient and its standard deviation. The position on the circumference of the tube is given by the angle θ subtended at the centre of the circle relative to the stagnation point with the clockwise direction positive. The peaks of the fluctuating values are mainly due to the vortex shedding which was investigated more particularly for the two cylinder case.

The Strouhal number versus the yaw angle for this configuration is given in Figure 9. This is the same for both tubes and it was shown that the alternate shedding is exactly in phase when the tubes are in alignment. The downstream tube is strongly subjected to the vortices which are shed by the upstream cylinder (see $\beta = 0$ at $\theta = 45°$ in Figure 6) and
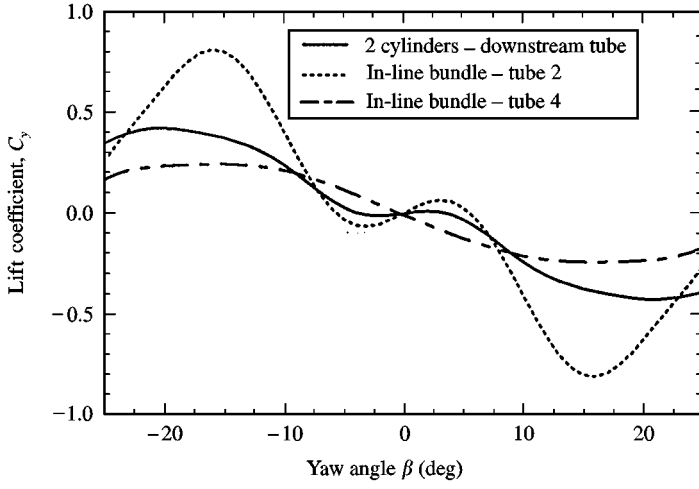
Figure 5. Lift coefficient versus yaw angle.
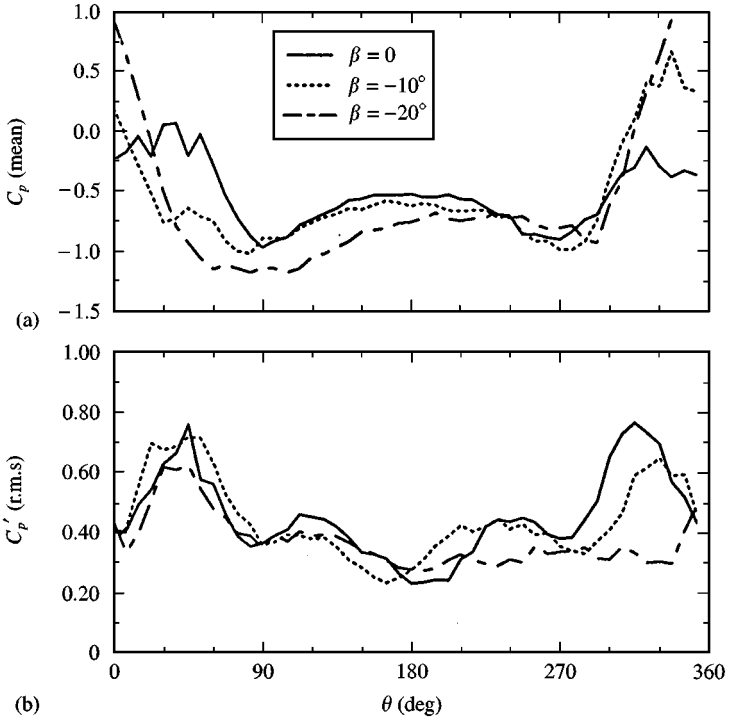
Figure 6. Pressure coefficient for the downstream tube of the two cylinder case: (a) mean value; (b) standard deviation.
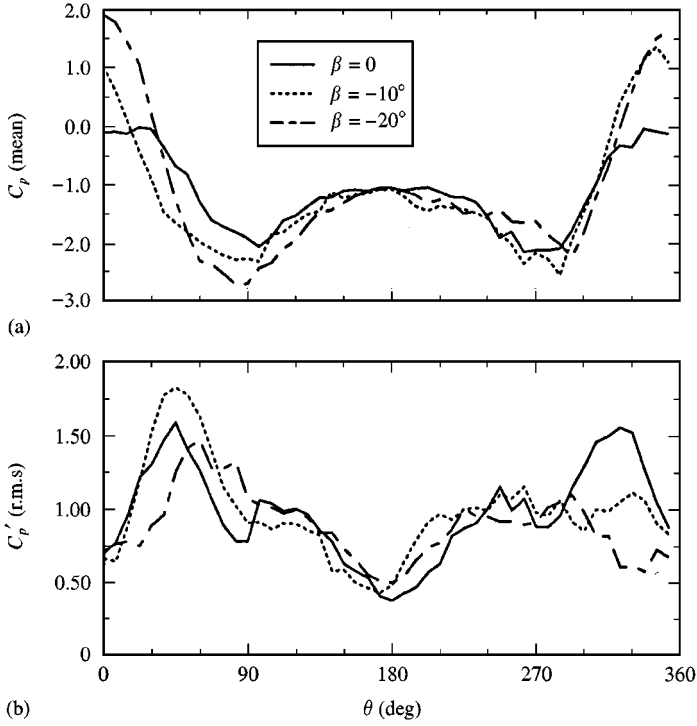
Figure 7. Pressure coefficient for tube 2 of the in-line bundle: (a) mean value; (b) standard deviation.
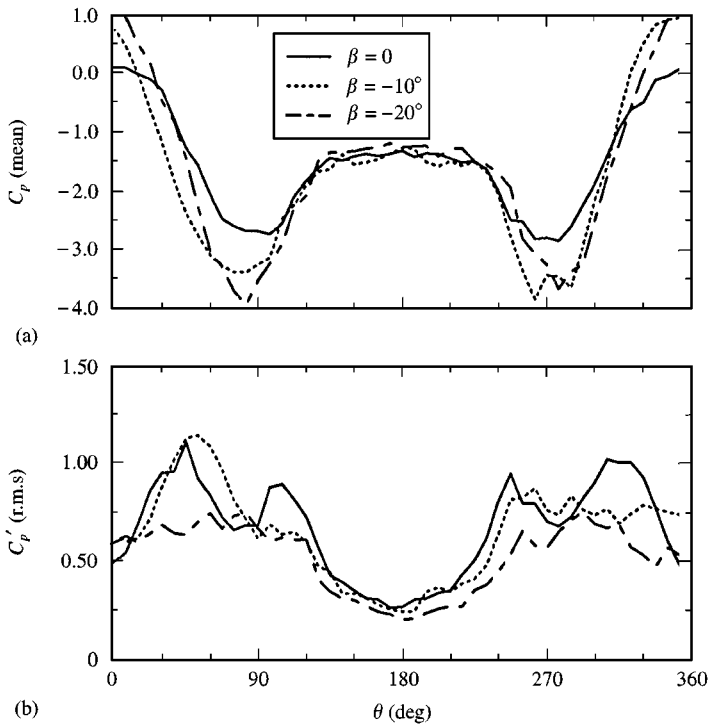
Figure 8. Pressure coefficient for tube 4 of the in-line bundle: (a) mean value; (b) standard deviation.
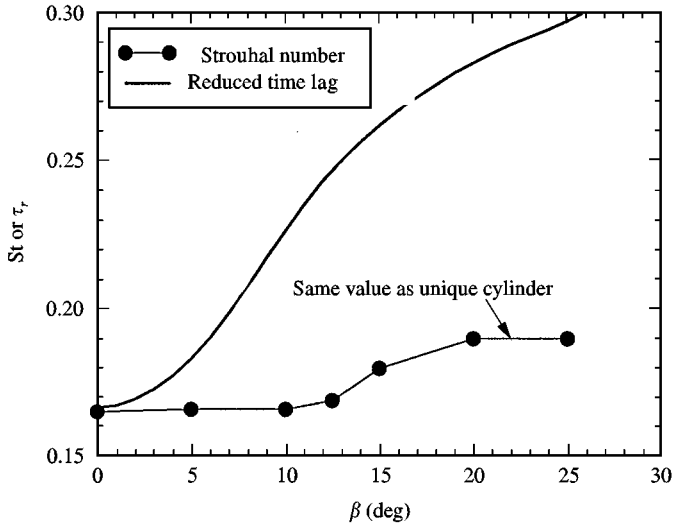
Figure 9. Strouhal number and reduced time lag for the case of two cylinders downstream tube.

weakly affected by its own shedding (at $\theta = 120°$). When the tubes are yawed at about $20°$, the shedding is no longer correlated and the Strouhal number returns to the value for the isolated cylinder. Note that for a spacing ratio (L/D) of 3 the downstream tube comes out of the shadow of the upstream cylinder at a yaw angle of $18.4°$.

The interesting point here is that the Strouhal number is related to the convection velocity of the alternate vortices. In particular, in the tandem position of the two cylinders, the Strouhal number if 0.165, which also corresponds to the value of the reduced time lag when it is calculated with equations (14) and (15), as reported in Figure 9. This coincidence has not yet been explained, but it is close to our physical intuition of the phenomenon.

Concerning the bundle, an almost constant Strouhal number between 0.23 and 0.24 was found inside the bundle, whatever the yaw angle. This value is similar to that given by the empirical relation of Weaver mentioned in Chen (1987) which, in the present case, gives a value of 0.25.

5. RESULTS OF NUMERICAL PREDICTIONS

The numerical predictions are carried out by solving equation (2) with the finite-difference scheme given in Appendix 1, which is chosen for its good accuracy and properties in terms of numerical damping and phase error.

The main results are given in Figure 10; the maximum amplitude reached is normalised relative to the diameter and plotted versus the reduced velocity. The Scruton number of the computations is 0.1706, corresponding to a very low structural damping. Experimental results of Bokaian & Geoola (1984) for a similar case of two cylinders are also plotted. The vortex-shedding excitation obtained in the experiments is not predicted by the computations since this phenomenon is not included in the model.

In the case of two cylinders, the galloping instability of the downstream tube shows good agreement between predictions and experimental results, and in particular the critical velocity is very well predicted by equation (12). Tube 2 of the bundle, which has a similar lift force variation (see Figure 5), has a higher critical velocity and about the same amplitude of
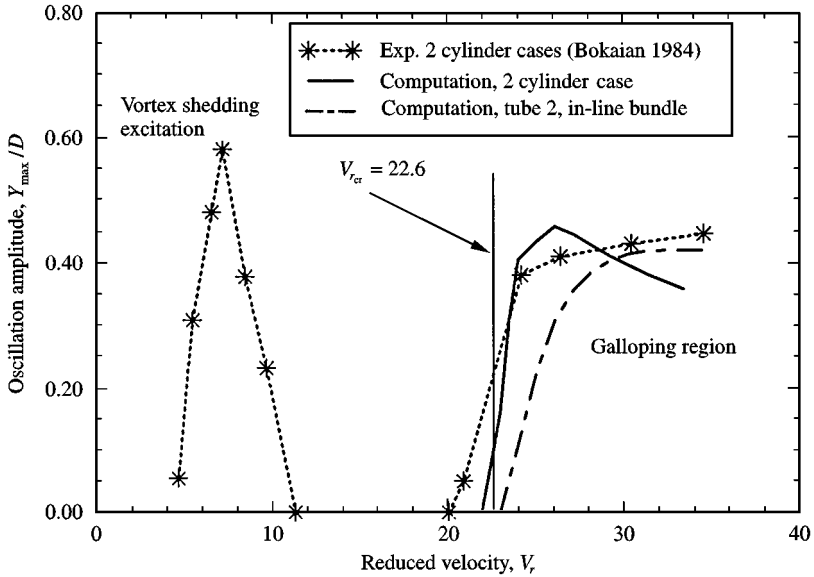
Figure 10. Amplitude of vibrations computed and comparison with experiments of Bokaian & Geoola (1984).

oscillations. On the other hand, tube 4 which is located far inside the bundle has a very different lift force and is not subject to galloping instability for the cases studied.

If we come back to the two-cylinder case, we observe limit-cycle amplitudes of the same order of magnitude in the experiments as in the computations. These amplitudes are of about half a diameter, in the range of the validity of the model. The agreement is less accurate than for the critical velocity and an effect of the Reynolds number is suspected here since it is not the same, varying from 2900 to 5800 in the experiments. This point is not completely clear. However, the agreement is quite good, and an analysis of the limit cycles is interesting in order to understand the dynamic behaviour of the system.

Typical detailed results are given in Figure 11. The phase plane [Figure 11(a)] of the movement shows a single loop, whereas the power spectrum of the displacement [Figure 11(b)] gives odd harmonic components of the fundamental frequency. This behaviour is due to the symmetry of the system studied, where the equilibrium position at yaw angle zero is a symmetrical centre. When we look at the hysteresis curve of the lift force [Figure 11(c)], we can see a large central loop which is circumscribed clockwise, i.e. there is a gain of energy, and two lateral loops that correspond to a loss of energy since they go anticlockwise. This type of force–displacement diagram is typical of the behaviour of interference galloping and shows the influence of the nonlinear aerodynamic damping which limits the amplitude of oscillations.

6. A DISCUSSION OF THE QUASI-STEADY ASSUMPTION

In the sense taken here, the quasi-steady assumption means that the steady aerodynamic coefficients used in the calculation are measured independently from the fact that the structure moves in the flow field. This assumption is therefore independent of the time lag concept and only implies that the fluid velocity is large enough for it not to detect the motion of the structure. Such a condition is classically given by the low-frequency
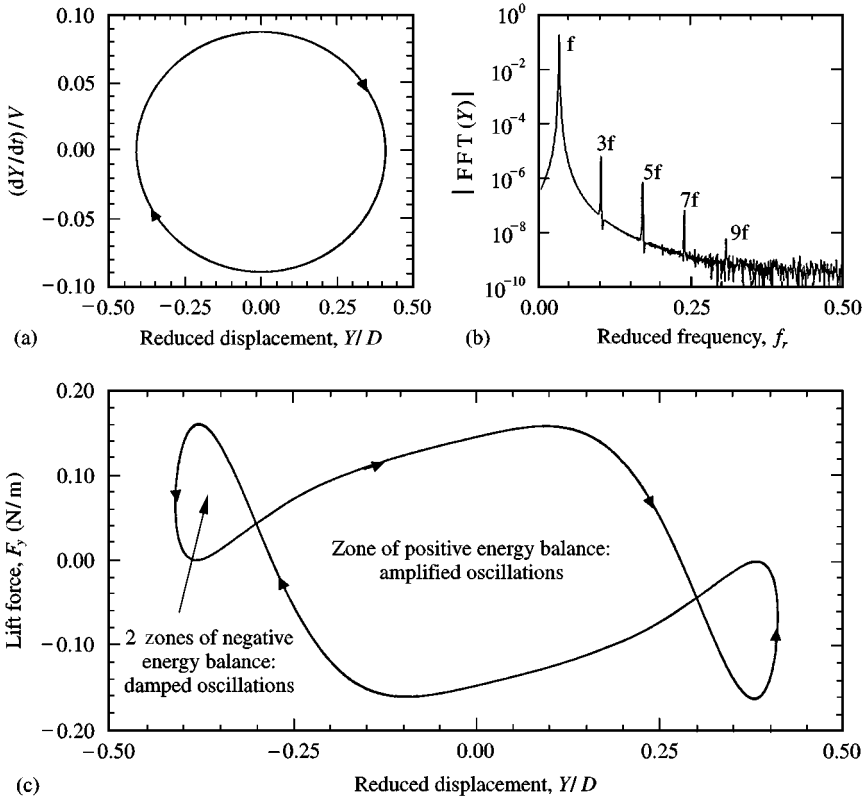
Figure 11. Limit cycle analysis for the case of two cylinders. (a) phase plan, (b) power spectrum of the displacement, (c) force–displacement diagram. Computation at $V_r = 29$.

assumption, i.e.

$$f_r = \frac{fD}{V} \ll 1. \qquad (16)$$

However, in the case of tube arrays, the motion considered is in the cross-flow direction, with a mean amplitude $\dot{y}'$ (root-mean-square of $\dot{y}$) and a mean flow velocity U_C for the downstream cylinder. If we assume a sinusoidal movement such as in equation (10), then the low reduced frequency assumption can be written as

$$\frac{\dot{y}'}{U_C} \approx \frac{4\pi f y_M}{\sqrt{2V}} \ll 1, \qquad (17)$$

where it has been assumed that U_C is close to $\frac{1}{2}V$, which is valid for our case because

$$\frac{U_C}{V} = \frac{L}{D}\tau_r \qquad (18)$$

by definition, and $\tau_r = 0.166$ as in Figure 9. This value of U_C should be corrected for other values of tube spacing ratio: in particular, small L/D ratios may lead to much smaller values of U_C. The main consequence is that the low reduced frequency assumption, as understood here, cannot be valid when the tube spacing ratio is too small.

The other limitation to the assumption is given by the motion amplitude that should not be too high. Nevertheless, the numerical application to this study of relation (17) gives, for an amplitude y_M equal to half a diameter, a value of 0·22 which is significantly smaller than 1.

Another point related to the conventional quasi-steady theory is the fact that the suggested time lag depends on the flow velocity. It introduces into the aeroelastic force model a dependence on the reduced frequency, even for linearized terms. This is not the case for the pure quasi-steady theory. Nevertheless, it is not easy to make a direct link between the present model and others such as Simpson's (Simiu & Scanlan 1986), though their physical behaviour seems to be similar on this particular point.

7. CONCLUSION

An improvement is suggested to the time-delayed quasi-steady model for the prediction of vibrations of aligned tubes. A physical interpretation of the time lag leads to a new expression based on static force coefficients. There is no empirical coefficient to adjust and the model is very convenient to use. The critical velocity is also deduced and comparison with available experimental results shows very good agreement with the present model.

An analysis of the limit cycles shows that the nonlinear behaviour of the dynamical system is similar to a Van der Pol oscillator with amplitudes of oscillation limited by nonlinear damping.

The model has a range of validity which can be summarized in two main points: (i) the low reduced frequency condition is given by inequality (17), which also implies limited amplitudes of oscillation; (ii) the tube spacing ratio cannot be too small a validation was given for $L/D = 3$; it seems possible to increase the distance but more difficult to decrease it.

An extension of this model was suggested in Bourdeix et al. (1997) to take into account the longitudinal displacement and the 3-D effects in a simplified manner. A few points remain unclear, especially the coincidence between the Strouhal number and the reduced time lag. Besides, the Reynolds number effect has not been investigated sufficiently. It would also be interesting to study the effect of the movement of upstream tubes, mainly in the case of a bundle which in fact represents the industrial application of this work.

ACKNOWLEDGEMENTS

REFERENCES

BLAZIC-BOROWA, E. & FLAGA, A. 1997 Numerical analysis of interference galloping of two identical circular cylinders at unsteady air onflow. *Proceedings of 2nd European and African Conference on Wind Engineering*, pp. 1815–1822, Genova, Italy, June 22–26.

BLEVINS, R. D. 1990 *Flow-Induced Vibrations*, 2nd edition, pp. 161–185. New York: Van Nostrand Reinhold.

BOKAIAN, A. & GEOOLA, F. 1984 Wake-induced galloping of two interfering circular cylinders. *Journal of Fluid Mechanics*, **146**, 383–415.

BOURDEIX, M. T., HEMON, P. & SANTI, F. 1997 Wind induced vibrations of chimneys using an improved quasi-steady theory for galloping. *Proceedings of 2nd European and African Conference on Wind*

Engineering, pp. 1351–1358, Genova, Italy, June 22–26. To appear in *Journal of Wind Engineering and Industrial Aerodynamics*.

CHABART, O. & LILIEN, J. L. 1997 Galloping of electric lines in wind tunnel facilities. *Proceedings of 2nd European and African Conference on Wind Engineering*, pp. 1751–1758, Genova, Italy, June 22–26.

CHEN, S. S. 1987 *Flow-Induced Vibrations of Circular Cylindrical Structures*. Berlin: Springer-Verlag.

DEN HARTOG, J. P. 1934 *Mechanical Vibrations*. New York: McGraw-Hill. Dover edition, 1985.

DE VOGELAERE, R. 1955 A method for the numerical integration of differential equations of second order without explicit first derivatives. *Journal of Research of NBS* **54**, No. 3, 119–125.

DIELEN, B. & RUSCHEWEYH, H. 1995 Mechanism of interference galloping of two identical circular cylinders in cross flow. *Journal of Wind Engineering & Industrial Aerodynamics*, **54/55**, 289–300.

FU, C. C. 1970 A method for the numerical integration of the equations of motion arising from a finite element analysis. *Journal of Applied Mechanics* **37**, 599–605.

FUNG, Y. C. 1955 *An Introduction to the Theory of Aeroelasticity*. New York: McGraw-Hill. Dover edition, 1993.

GRANGER, S. & DE LANGRE, E. 1995 Flow vibrations and dynamic instability of heat exchanger tube bundles (in french). *Revue Française de mécanique*, **1995–1**, 37–47.

GRANGER, S. & PAÏDOUSSIS, M. P. 1996 An improvement of the quasi-steady model with application to cross-flow vibration of tube arrays. *Journal of Fluid Mechanics*, **320**, 163–184.

HÉMON, P. 1997 Modélisation de l'interférence de galop de cylindres circulaires en écoulement transverse. *Comptes Rendus de l'Académie des Sciences de Paris* **324**, Série IIb, 611–618.

KERN, G. & MAITZ, A. 1997 Self-excited wind-induced vibrations and limit cycles in bundled conductors. *Proceedings of 2nd European and African Conference in Wind Engineering*, pp. 1743–1750, Genova, Italy, June 22–26.

KNISELY, C. W. & KAWAGOE, M. 1988 Force-displacement measurements on closely spaced tandem cylinders. In *Proceedings of the First International Colloquium on Bluff Body Aerodynamics and its Applications*, pp. 81–90, BBAA I, Kyoto, Japan, October 17–20.

PRICE, S. J. & PAÏDOUSSIS, M. P. 1984 An improved mathematical model for the stability of cylinder rows subject to cross-flow. *Journal of Sound and Vibration*, **97**, 615–640.

SIMIU, E. & SCANLAN, R. H. 1986 *Wind Effects on Structures*, 2nd edition. New York: Wiley & Sons.

WU, R. W.-H. & WITMER, E. A. 1973 Stability of the De Vogelaere Method for Timewise Numerical Integration. *AIAA Journal* **11**, 1432–1436.

ZDRAVKOVICH, M. M. 1987 Review of interference-induced oscillations in flow past two parallel circular cylinders in various arrangements. *Proceedings of the 7th International Congress on Wind Engineering*, pp. 183–199, Aachen, Germany, July 6–10.

APPENDIX 1: THE NUMERICAL SCHEME

This scheme was first suggested by De Vogelaere (1955) and then improved by Fu (1970). The original scheme is adapted here is order to obtain a predictor-corrector algorithm. The aim is to solve an expression of the form $\ddot{x} + c\dot{x} = G(t, x, \dot{x})$.

Initial values:

$$G_0 = G(t_0, x_0, \dot{x}_0),$$

$$x_{-1/2} = x_0 - \frac{\Delta t}{2}\dot{x}_0 + \frac{\Delta t^2}{8}(G_0 - c\dot{x}_0),$$

$$G_{-1/2} = G(t_{-1/2}, x_{-1/2}, \dot{x}_0),$$

$$\dot{x}_{-1/2} = \frac{1}{4 - c\Delta t}((4 + c\Delta t)\dot{x}_0 - \Delta t(G_{-1/2} + G_0)).$$

Prediction half time step:

$$x^*_{n+1/2} = x_n + \frac{\Delta t}{2}\dot{x}_n + \frac{\Delta t^2}{24}(4G^*_n - G_{n-1/2} - c(4\dot{x}_n - \dot{x}_{n-1/2})),$$

$$G^*_{n+1/2} = G(t_{n+1/2}, x_{n+1/2}, \dot{x}_n),$$

$$\dot{x}^*_{n+1/2} = \frac{4}{4 + c\Delta t}\left(\dot{x}_n + \frac{\Delta t}{4}(G^*_n + G^*_{n+1/2} - c\dot{x}_n)\right).$$

Correction half time step:

$$x_{n+1/2} = x_n + \frac{\Delta t}{2}\dot{x}_n + \frac{\Delta t^2}{24}(2G_n - 2c\dot{x}_n + G^*_{n+1/2} - c\dot{x}^*_{n+1/2}),$$

$$\dot{x}_{n+1/2} = \frac{4}{4 + c\Delta t}\left(\dot{x}_n + \frac{\Delta t}{4}(G_n + G^*_{n+1/2} - c\dot{x}_n)\right),$$

$$G_{n+1/2} = G(t_{n+1/2}, x_{n+1/2}, \dot{x}_{n+1/2}).$$

Time step:

$$x_{n+1} = x_n + \Delta t\dot{x}_n + \frac{\Delta t^2}{6}(G^*_n + 2G_{n+1/2} - c(\dot{x}_n + 2\dot{x}_{n+1/2})),$$

$$G^*_{n+1} = G(t_{n+1}, x_{n+1}, \dot{x}_{n+1/2}),$$

$$\dot{x}_{n+1} = \frac{6}{6 + c\Delta t}\left(\dot{x}_n + \frac{\Delta t}{6}(G^*_{n+1} + 4G_{n+1/2} + G^*_n - c(4\dot{x}_{n+1/2} + \dot{x}_n))\right).$$

This fourth-order scheme has a stability condition $\Delta t\omega \leqslant 2\sqrt{2}$ studied by Wu & Witner (1973). It has no numerical damping and the phase error is at least of order 4.

APPENDIX 2: NOMENCLATURE

$C_p = P - P_{atm}/Q$	mean pressure coefficient
C'_p	fluctuating pressure coefficient
$C_x = F_x/DQ$	drag force coefficient
$C_y = F_y/DQ$	lift force coefficient
D	tube diameter (m)
f	frequency of the structure (Hz)
$f_r = fD/V$	reduced frequency
f_v	frequency of vortex shedding (Hz)
F_x, F_y	aerodynamic forces of x- and y-axis (N/m)
L	tube spacing (m)
m	mass per unit length (kg/m)
P	pressure (Pa)
P_{atm}	atmospheric pressure (Pa)
$Q = \frac{1}{2}\rho V^2$	dynamic pressure (Pa)
$Re = VD/v$	Reynolds number
$Sc = 2\eta m/\rho D^2$	Scruton number
$St = f_v D/V$	Strouhal number
t	time (s)
U_C	convection velocity (m/s)
V	upstream flow velocity (m/s)
$V_r = V/fD = 1/f_r$	reduced velocity
y	tube displacement (m)
β	yaw angle (deg)
η	reduced damping (refered to critical damping)
v	kinematic viscosity (m^2/s)
ρ	fluid density (kg/m^3)
τ	time lag (s)
$\tau_r = D/\tau V$	reduced time lag
$\omega = 2\pi f$	angular velocity (rad/s)

Subscripts

a	related to relative velocity
P	related to position
0	related to an equilibrium position
$\cdot$	denotes time derivative